Root Cracking Modes in Restraint Cracking Test of High Strength Steel Based on AE Technique and Fractography †

Fukuhisa MATSUDA*, Hiroji NAKAGAWA** and Yoshinori MORIMOTO***

Abstract

Restraint cracking tests were applied against weldable high strength steels whose ultimate strengths are 80 and 90 kg/mm² class. Shielded metal-arc welding was done in Y-, y- or single bevel groove in the test specimens, and AE linear source location technique along the weld line was started immediately after the welding and continued for 48 hrs. Cracked surface was studied in detail with SEM ater the test. Consequently, combination of AE technique and fractography revealed that there is distinct difference in root cracking mode in relation to whether the cracking mainly passed through heat-affected zone or weld metal. The root cracking occurred in heat-affected zone has a tendency to grow along the weld line close to the bottom of weld bead instead of upward growth toward the surface of weld bead. On the other hand, the root cracking occurred in weld metal has a tendency to grow toward the surface of weld bead due to anisotropy of columnar crystal.

KEY WORDS: (Acoustic Emission) (High Strength) (Cold Cracking) (Hydrogen Embrittlement) (Fractography)

1. Introduction

Root cracking is one of serious problems in welding of high strength steels. The cracking condition is generally discussed with variables, such as diffusible hydrogen content, residual hydrogen content[1], cooling time, restraint intensity, and so on. These variables, however, are generally not constant along the weld line. Moreover, anisotropy effect of columnar crystal in weld metal[2] may have remarkable influence on the root cracking behavior in weld metal. So, it is very interesting to reveal where the root cracking initiates from and grow in actual weld.

The authours have studied these problems in previous papers[3−5] using AE source location technique against restraint cracking tests. In these papers, also macroscopic fracture analysis on the cracked surface and its microscopic fracture analysis with scanning electron microscope (SEM) have been used jointly, since AE source location along thickness direction of test specimen is now impossible. Consequently, combination of these techniques have revealed interesting behaviors of root cracking. Thus, this paper summarizes the results obtained in the previous papers[3−5].

2. Materials Used and Experimental Procedures

2.1 *Materials used*

Weldable heat-treated high strength steels whose ultimate strengths were 80 and 90 kg/mm² class were used for the restraint cracking tests. In this paper, the former is designated as HT80 and the latter as HY110. The chemical composition of HT80 is T-1 type and that of HY110 is 4Ni-Cr-Mo-V type. The configurations of specimens for restraint cracking tests are shown in **Fig. 1**, in which a Y-, y- or single bevel groove was machined. As regards HT80 with single bevel groove, the groove length L was changed in order to obtain various restraint

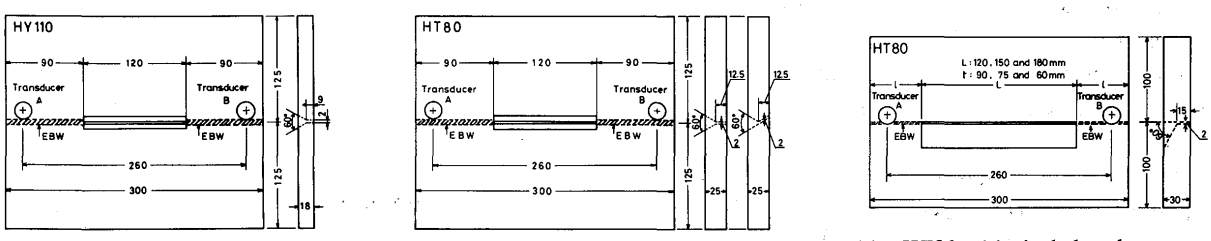

(a) HY110 with Y-groove (b) HT80 with Y- or y-groove (c) HT80 with single bevel groove

Fig. 1 Specimen configuration of restraint cracking test

† Received on April 4, 1980

* Professor
** Research Instructor
*** Graduate Student (Presently, Komai Iron Works Co. LTD)

Transactions of JWRI is published by Welding Research Institute of Osaka University, Suita, Osaka, Japan

intensity. The restraint welding in both sides of the groove was done with electron beam welding by each one pass from top and back surfaces. The restraint intentities in the middle of the groove length of the all specimens are summarized in **Table 1**, which were calculated using a formula[6] in case of uniformly distributed load.

Table 1 Calculated restraint intensities of test specimens

Material	Groove shape	Groove length (mm)	Restraint intensity (kg/mm·mm)
HY110	Y	120	1200
HT80	single bevel	120	1800
		150	1100
		180	600
	Y, y	120	1600

2.2 *Welding procedure*

Test welding was done with shielded metal-arc welding. Electrode used in HT80 was JIS D8016 (corresponding to AWS E11016) class and tentative electrode in HY110. The ultimate strength of the deposited metal of the tentative electrode was about 100 kg/mm^2. Total number of the test specimens was 42, and baking condition of the electrode and the preheating temperature of the test specimen was varied in order to obtain various crack sizes. The starting part and the crater of the weld bead were turned away from the root gap to avoid welding defects. The welding condition was 170A, 25V, 150 mm/min and thus 17kJ/cm. Slags on the surface of weld bead were completely removed immediately after the welding.

2.3 *Procedure of AE measurement*

The AE monitoring system used was Dunegan/Endevco 3000 series which had dual channels and thus had a capability of linear source location[7]. The AE transducers used were differential type having flat response and sensitivity of −84dB referred to 1V/μbar, the bandpass filters were selected from 100 to 350kH$_Z$, and the total gain was set to 70dB. The relative error of AE source location in this AE monitoring system was within 10 (%) from actual crack location[7].

Two AE transducers were set on the test specimen as shown in Fig. 1 and AE measurement was started from 2min after the completion of welding. The temperature of weld metal at this moment was about 70°C without preheating condition. The AE measurement was continued for 48hrs.

2.4 *Observation of cracked surface*

After the AE measurement, the test specimen was immediately taken into an electric furnace of about 350°C in order to oxidize the cracked surface, though the oxidizing treatment was omitted as regards fully cracked specimen. Subsequently the test specimen was fractured by a bending test machine at room temperature. Then the distribution of cracks was observed in detail with naked eyes and a stereomicroscope, and crack ratios defined in the following were measured on the fracture surface. Crack ratio Ca was defined as follows:

$$Ca = A_c/A_s \times 100\ (\%) \quad \ldots\ldots\ldots \quad (1)$$

where, A_c; cracked area

A_s; sum of cracked and fractured areas.

Crosssectional crack ratio C_S was defined as follows:

$$C_S = \frac{1}{N}\sum^{N} H_c/H_b \times 100\ (\%) \quad \ldots\ldots \quad (2)$$

where, N ; measured number (selected to five in equal distance for the weld bead)

H_c; height of root crack in crosssection.

H_b; height of weld bead in crosssection.

Surface crack ratio C_f was defined as follows:

$$C_f = \Sigma L_f/L \times 100\ (\%) \quad \ldots\ldots\ldots \quad (3)$$

where, ΣL_f; total length of cracks on the surface of weld metal

L; length of weld bead.

Root crack ratio C_r was defined as follows:

$$C_r = \Sigma L_r/L \times 100\ (\%) \quad \ldots\ldots\ldots \quad (4)$$

where, ΣL_r; total length of cracks at the bottom of weld bead.

Moreover, the cracked surface was studied in detail with a scanning electron microscope (SEM) as regards fully cracked specimen.

3. Experimental Results and Discussions

3.1 *Characteristic of crack path in transverse crosssection*

Crack path in transverse crosssection of welded zone of fully cracked specimen is summarized in **Fig. 2**. The root cracking in HY110 generally passed through the weld metal, though it ocurred in the heat-affected zone in slightly cracked specimen[4]. The root cracking in HT80 with single bevel groove passed through the heat-affected zone except for the shear lip zone into the weld metal,

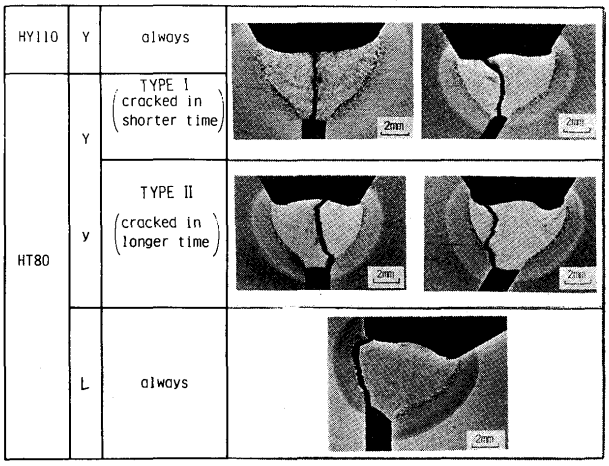

Fig. 2 Path of root cracking in transverse crosssection of welded zone. ⌐ means single bevel groove.

though the root cracking in the specimen with the highest restraint intensity passed from the heat-affected zone into the weld metal before turning as the shear lip zone[3]. The path of the root cracking in HT80 with Y- or y-groove was classified into two types irrespective of Y- or y-groove. That is, the root cracking in Type I generally passed through only the weld metal, as in HY110 and that in Type II passed in the heat-affected zone to a certain extent and then turned into the weld metal before the final stage resulting in the formation of shear lip zone. Insufficient baking condition of electrode generally had a tendency to result in Type I, and thus the test specimen in Type I completely cracked in comparatively shorter period than that in Type II. The cracking path has been described in detail elsewhere (Refs. 3, 4 and 5).

3.2 Root cracking mode based on AE and fractography

Root cracking mode estimated with AE and fractography was clearly related with the crack path shown in Fig. 2, as next mentioned. Typical examples of the AE behavior in each case in Fig. 2 are shown in **Fig. 3**, which gives the change in AE source location during the cracking test. Relative location in the abscissa is defined to be 0 (%) at the left AE transducer and 100 (%) at the right one in Fig. 1, and the increase in the relative location agrees with the welding direction. Considering the error in AE source location in the AE monitoring system[7], the AE from the weld should lie in the region indicated by arrows.

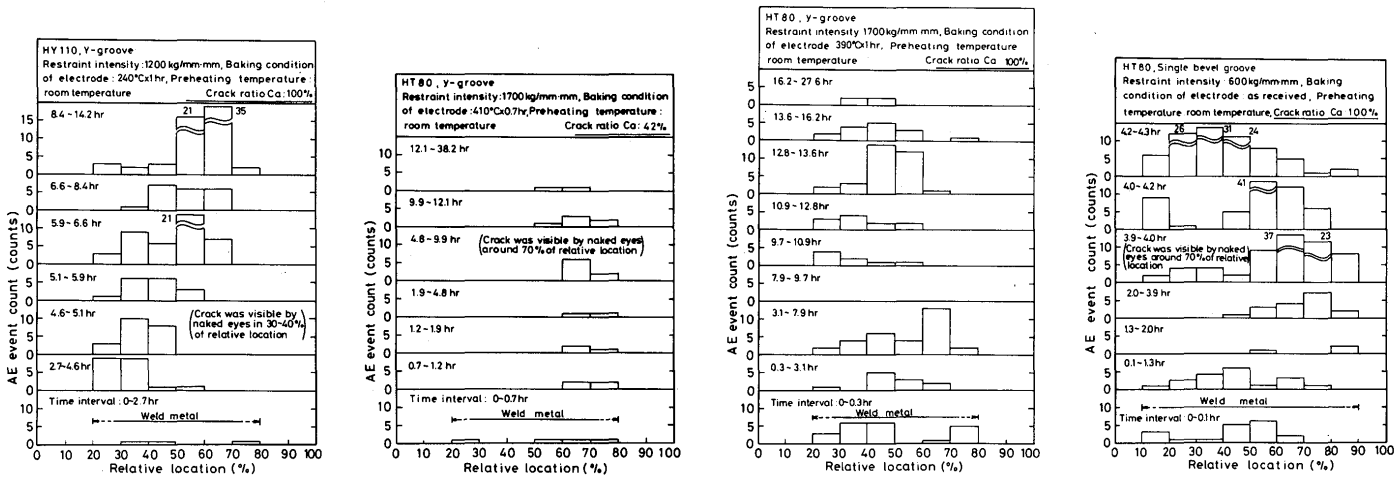

(a) HY110 with Y-groove (b) Type I of HT80 with y-groove (c) Type II of HT80 with y-groove (d) HT80 with single bevel groove

Fig. 3 Typical examples of change in AE source location vs. time

Comparing Fig. 3 (a) with Fig. 3 (d) which are typical examples of root cracking in weld metal and heat-affected zone respectively, namely in HY110 and HT80 with single bevel groove, the AE events in Fig. 3 (a) had a tendency to concentrate to about 30 (%) of the relative location until the cracking became visible on the surface of weld bead, whereas the AE events in Fig. 3 (d) occurred from place to place over the whole length of weld bead. These suggest that the root cracking in Fig. 3 (a) grew upwards locally to the surface of weld bead, and that the root cracking in Fig. 3 (d) had already extended over the whole weld length near the bottom of weld bead by the time when the cracking became visible on the surface of weld bead.

Fig. 3 (b) shows the typical example of Type I in HT80 with Y- or y-groove, where the same tendency as in Fig. 3 (a) is observed. Fig. 3 (c) shows the typical example of Type II in HT80 with Y- or y-groove, where the same tendency as in Fig. 3 (d) is observed, though a distinct temporary cessation of AE is observed between

7.9 and 9.7hr as a differnece from Fig. 3 (d). The cessation continued as long as 10hr on a certain occasion[5]. This temporary cessation of AE is considered to be an incubation period when the root cracking in the heat-affected zone turns into the weld metal[5], because it is considered that still more enrichment of diffusible hydrogen to the crack tip is required for the cracking growth into the weld metal due to the lower hardness in the weld metal than in the heat-affected zone. The behavior of AE in each case in Fig. 3 has been described in detail elsewhere (Refs. 3, 4 and 5).

The macrofractographs and their sketches of the

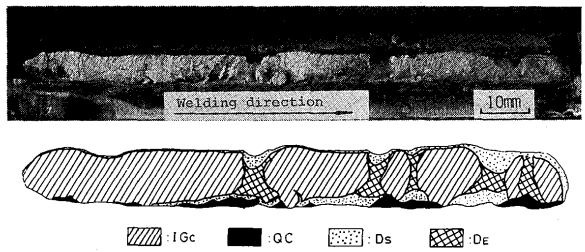

(a) HY110 with Y-groove

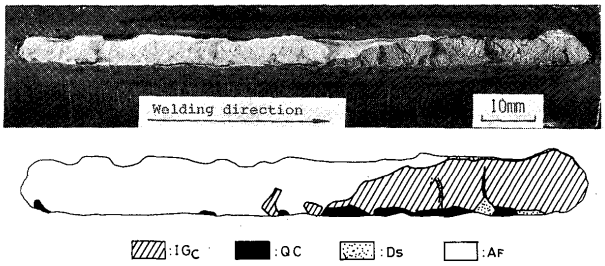

(b) Type I of HT80 with y-groove

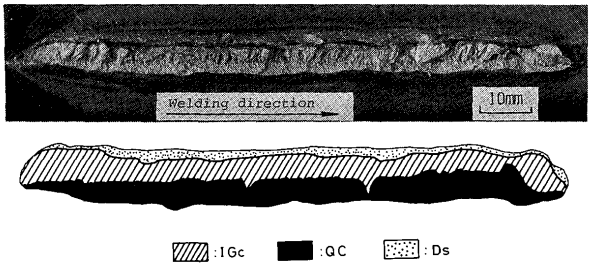

(c) Type II of HT80 with y-groove

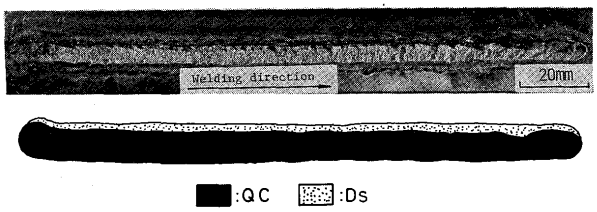

(d) HT80 with single bevel groove

Fig. 4 Macrofractographs of specimens in Fig. 3

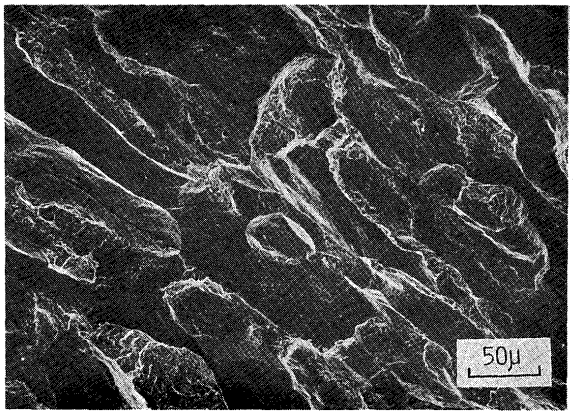

(a) IGc (mainly intergranular)

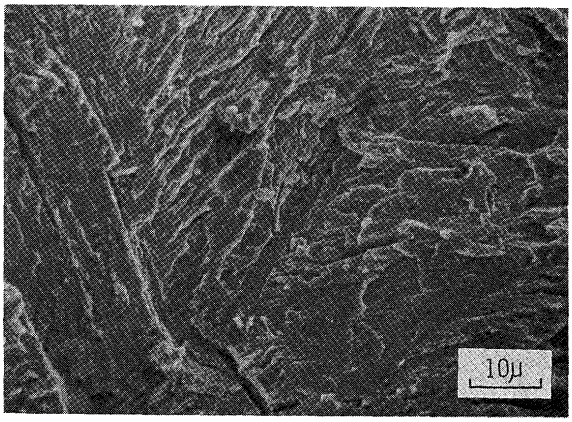

(b) QC (mainly quasi-cleavage)

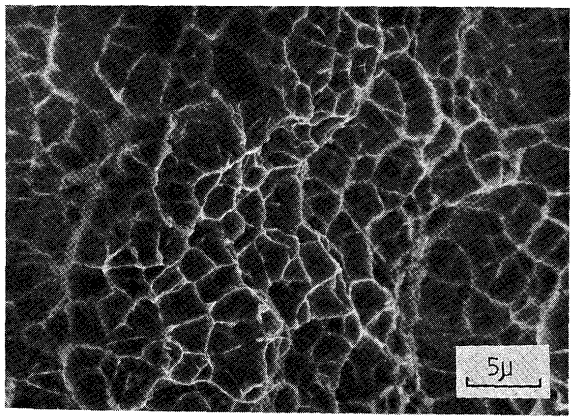

(c) D_E (equiaxed dimple)

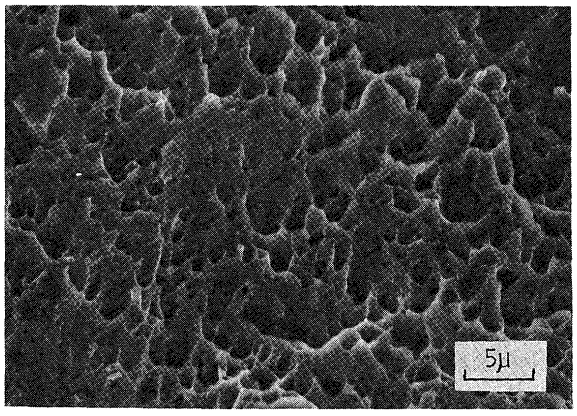

(d) Ds (shear dimple)

Fig. 5 Typical microfractographs of root crack obtained with SEM

specimens in Fig. 3 are summarized in **Fig. 4**, where the marks IGc, QC, D_E and D_s show the regions which gave characteristic surface in SEM observation. Their microscopic features with SEM are shown in **Fig. 5**. The IG_C region, Fig. 5 (a), was mainly composed of intergranualr fracture along columnar crystal of prior austenite and partly of quasi-cleavage affected by hydrogen. The IG_C region was formed in the weld metal. The QC region, Fig. 5 (b), was mainly composed of quasi-cleavage affected by hydrogen and slightly of non-directional intergranular fracture. The QC region was formed in the heat-affected zone. The D_E region, Fig. 5 (c), was composed of equiaxed dimple of equiaxed dimple fracture, and the D_S region, Fig. 5 (d), was composed of shear dimple fracture. Both the D_E and D_S regions were formed in the weld metal. By the way, A_F region in Fig. 4 (b) is artificially fractured region after the cracking test. Comparing Fig. 4 with Fig. 3, it is imagined that one of the reasons of the differnece in the root cracking mode discussed in Fig. 3 arises from anisotropy of cracking along columnar crystal in weld metal.

The difference in the root cracking mode above mentioned is also confirmed in **Fig. 6**, which shows the change in crack ratios C_s, C_r and C_f vs. C_a in Types I and II of

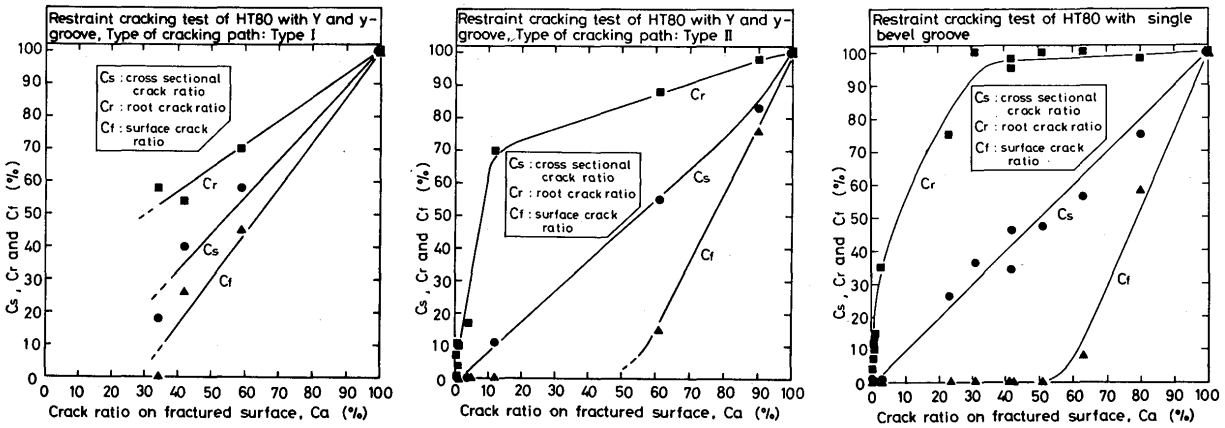

(a) Type I of HT80 with Y- and y-groove (b) Type II of HT80 with Y- and y-groove (c) HT80 with single bevel groove.

Fig. 6 Change in crack ratios C_s, C_r and C_f vs. C_a

HT80 with Y-and y-groove and in HT80 with single bevel groove. In each figure, especially in Figs. 6 (b) and (c), C_s nearly equal to C_a. However, the behaviors of C_r and C_f in Figs. 6 (b) and (c) are quite different from those in Fig. Fig. 6 (a). That is to say, in Figs. 6 (b) and (c) C_r increases steeply between 0 and 10 (%) of C_a, and C_f increases steeply from about 60 (%) of C_a. These behaviors also suggest that the root cracking in the heat-affected zone has a tendency in early stage to grow along the weld line close to the bottom of weld bead instead of the upward growth toward the surface of weld bead. On the other hand, in Fig. 6 (a) C_r is only about 1.5 times as larger as C_a at the most, and C_f increases from about 40 (%) of C_a. These behaviors suggest that the root cracking in the weld metal has a tendency to grow toward the surface of weld bead.

Then, **Table 2** shows the locations where the root cracking was first visible on the surface of weld bead in HT80 with Y-, y- and single bevel groove. The results mean that the location shifted from the vicinity of crater to the middle of weld length together with the increase in the restraint intensity. **Figure 7** shows macrofractographs, where cracked parts were oxidized, of HT80 with single bevel groove in which the root cracking stopped naturally. Almost all the vicinity of the bottom of weld bead already cracked in every macrofractograph, and it is noticed that the location where the cracking grew farthest from the bottom shifted from the vicinity of crater to the middle of weld length together with the decrease in groove length i.e. increase in the restraint intensity. This tendency well agrees with that in Table 2.

Table 2 Location where root cracking was first visible on surface of weld bead in HT80

Groove shape	Restraint intensity (kg/mm·mm)	Location of cracking emergence
single bevel	600	vicinity of crater
	1100	middle part of weld length*
	1800	middle part of weld length
Y, y	1700	vicinity of crater or middle part

* there was only one datum.

Now, a brief discussion on this tendency mentioned in Table 2 and Fig. 7 is tried in the following. **Table 3** shows residual hydrogen content at 100(°C) in welded zone near

(a) groove length: 180mm, crack ratio: 42(%)

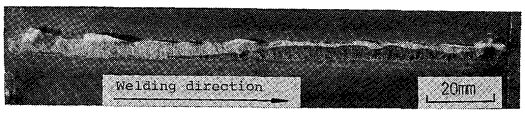

(b) groove length: 150mm, crack ratio: 42(%)

(c) groove length: 120mm, crack ratio: 31(%)

Fig. 7 Distribution of root cracking in HT80 with single bevel groove

Table 3 Calculated hydrogen content at 100(°C) in welded zone in the case when initial hydrogen content is unity

Location	Residual hydrogen content
starting part	0.90
middle part	0.83
crater part	0.92

the starting part of welding, the middle part and the crater part calculated by empirical formula[1] using measured cooling curve in the weld metal. The result means that the residual hydrogen content near the starting part is nearly equal to that in the crater part and they are somewhat higher than that near the middle part. On the other hand, analytical formula[8] on restraint intensity in restraint cracking test by assuming instantaneous heat source shows the following tendency. That is, short groove length gives a distribution of restraint intensity which has a peak at the middel part, and long groove length gives a distribution which has peaks near the both starting and crater parts. While, it is shown[9] that effect of a moving heat source has a tendency to raise the restraint intensity near the crater part and to lower that near the starting part, and this tendency is remarkable in long groove length. Consideration of these factors brings a supposition that the cracking tendency shown in Table 2 and Fig. 7 is mainly caused by the distribution of restraint intensity, and hardly caused by the distribution of residual hydrogen content.

3.3 Illustration of root cracking mode

The root cracking modes mentioned above are summarized in **Fig. 8**, where cracks are illustrated with the

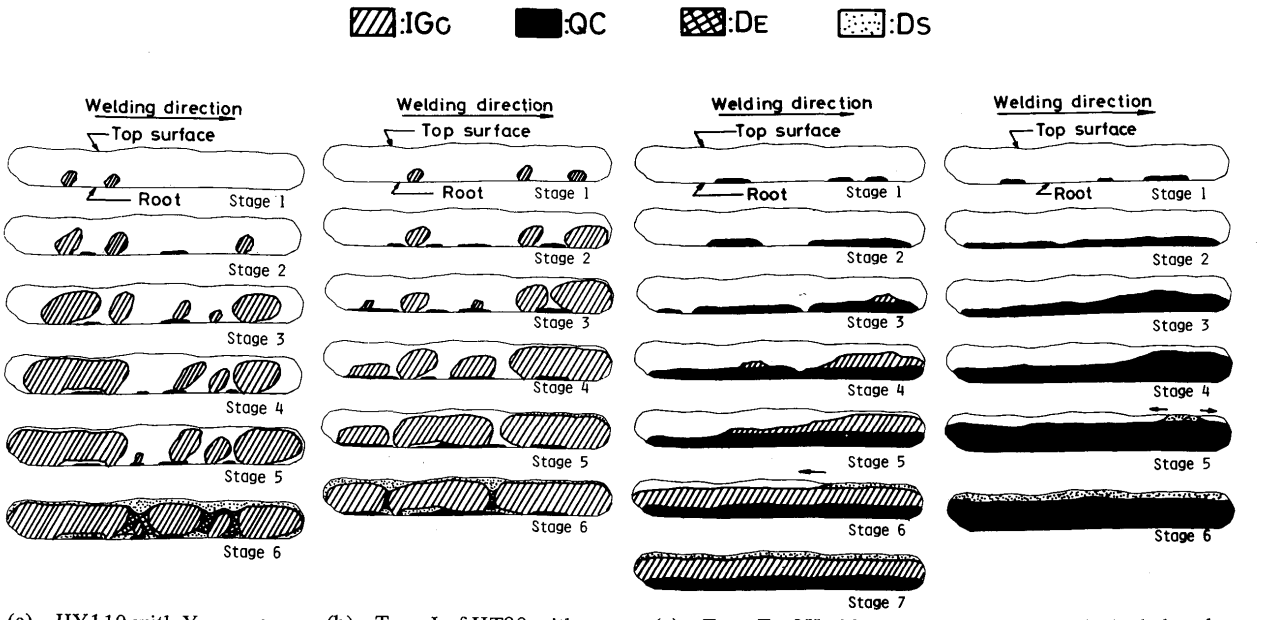

(a) HY110 with Y-groove (b) Type I of HT80 with Y- or y-groove (c) Type II of HT80 with Y- or y-groove (d) HT80 with single bevel groove

Fig. 8 Illustration of root cracking mode

same drawing as in Fig. 4. The root cracking in HY110 with Y-groove and Type I of HT80 with Y- or y-groove has a tendency to grow upwards like fan-shape[2] in weld metal due to anisotropy effect of columnar crystal. The root cracking in HT80 with single bevel groove and Type II of HT80 with Y- or y-groove has a tendency in early stage to grow in heat-affected zone along the weld line close to the bottom of weld bead. However, in Type

II of HT80 the root cracking growing in the heat-affected zone turns into the weld metal as IG_c mode due to the stress distribution accompanied with Y- or y-groove. On this occasion distinct temporary incubation period arises. Besides, groove length or distribution of restraint intensity affects overall distribution of cracking in each case to some extent. The reason why two types occur in HT80 with Y- or y-groove due to the difference in baking condition of electrode is a future subject, though it must be sure that the distribution of hydrogen concentration in the transverse crossection of welded zone is a major factor.

4. Conclusions

AE source location technique and fractography were utilized for studying the root cracking behavior in restraint cracking test. Main conclusions obtained are as follows:

(1) There is distinct difference in root cracking mode in relation to whether the cracking mainly passed through heat-affected zone or weld metal.

(2) The root cracking occurred in heat-affected zone has a tendency in early stage to grow along the weld line close to the bottom of weld bead instead of upward growth toward the surface of weld bead.

(3) The root cracking occurred in weld metal has a tendency to grow toward the surface of weld bead due to anisotropy of columnar crystal.

(4) When the root cracking growing in heat-affected zone turns into weld metal as seen in Y- or y-groove, temporary incubation period continues for 3 to 10hr.

(5) Groove length or distribution of restraint intensity affects overall distribution of root cracking to some extent.

References

1) K. Satoh, etal: J. Japan Weld. Soc., Vol. 48 (1979), No. 4, p. 248 (in Japanese).
2) F. Matsuda, et al: Trans. JWRI, Vol. 6 (1977), No. 2, p. 219.
3) F. Matsuda, et al: Trans. JWRI, Vol. 7 (1978), No. 2, p. 203.
4) F. Matsuda, et al: Trans. JWRI, Vol. 8 (1979), No. 1, p. 97.
5) F. Matsuda, et al: Trans. JWRI, Vol. 8 (1979), No. 2, p. 241.
6) Y. Ueda, et al: Trans. JWRI, Vol. 7 (1978), No. 1, p. 11.
7) F. Matsuda, et al: Trans. JWRI, Vol. 7 (1978), No. 1, p. 87.
8) Y. Ueda, et al: Preprints of National Meeting of JWS, No. 22, 1978, p. 142 (in Japanese).
9) Y Ueda, et al: J. Japan Weld. Soc., Vol. 44 (1975), No. 7, p. 580 (in Japanese).